

# Theory of Tunneling Effect in 1D AIII-class Topological Insulator (Nanowire) Proximity Coupled with a Superconductor

Ryoi Ohashi, Yukio Tanaka and Keiji Yada

Department of Applied Physics, Nagoya University, Nagoya 464-8603, Japan

We study the tunneling effect in an AIII-class insulator proximity coupled with a spin-singlet  $s$ -wave superconductor, in which three phases are characterized by the integer topological invariant  $\mathcal{N}$ . By solving the Bogoliubov–de Gennes equation explicitly, we analytically obtain a normal reflection coefficient  $R_{\sigma\sigma'}$  and an Andreev reflection coefficient  $A_{\sigma\sigma'}$ , and derive a charge conductance formula, where  $\sigma(\sigma')$  is the spin index of a reflected (injected) wave. The resulting conductance indicates a wide variety of line shapes: (i) gap structure without coherence peaks for  $\mathcal{N} = 0$ , (ii) quantized zero-bias conductance peak (ZBCP) with height  $2e^2/h$  for  $\mathcal{N} = 1$ , and (iii) ZBCP spitting for  $\mathcal{N} = 2$ . At zero bias voltage  $eV = 0$ ,  $\sum_{\sigma\sigma'} R_{\sigma\sigma'} = \sum_{\sigma\sigma'} A_{\sigma\sigma'}$  is satisfied and the spin direction of an injected electron is rotated at approximately  $90^\circ$  for the  $\mathcal{N} = 1$  state. Meanwhile,  $A_{\sigma\sigma'} = 0$  is satisfied for the  $\mathcal{N} = 2$  state, and the spin rotation angle can become  $180^\circ$ .

## I. INTRODUCTION

The tunneling effect in a normal metal/superconductor (N/S) junction has been considered to be a basic quantum phenomenon since the discovery of superconductivity. Blonder, Tinkham, and Klapwijk (BTK) established that tunneling conductance can be expressed by the coefficients of the Andreev reflection and normal reflection in ballistic junctions [1]. By extending the BTK theory, a conductance formula has been developed for unconventional superconductors [2, 3], where a pair potential changes sign on the Fermi surface and possesses the so-called surface Andreev-bound states (SABSs). This formula has clarified that the sharp zero-bias conductance peak (ZBCP) observed in many experiments of high  $T_C$  cuprate [4–10] stems from the zero energy surface Andreev-bound states (ZESABSs) [11–15] in unconventional nodal superconductors. Applying this formula for a spin-triplet chiral  $p$ -wave superconductor, a broad ZBCP has been obtained reflecting on the linear dispersion of the SABS [16–18]. This result is consistent with the tunneling experiments of  $\text{Sr}_2\text{RuO}_4$  [19, 20] and supports the realization of spin-triplet superconductivity in  $\text{Sr}_2\text{RuO}_4$  [21, 22].

It is known that the physical origin of these SABSs stems from the chiral edge state protected by the topological invariant defined in the bulk Hamiltonian [23–25], and the high  $T_C$  cuprate and  $\text{Sr}_2\text{RuO}_4$  are regarded as topological superconductors [26]. In the last decade, it has been established that topologically protected SABS can be generated based on a low-dimensional electron system with strong spin-orbit coupling without using unconventional pairings. For example, for the  $s$ -wave superconductor/ferromagnet junction on the surface of a topological insulator (TI), a chiral edge mode is generated similar to  $\text{Sr}_2\text{RuO}_4$ . Previously, one of the authors of this study, YT, derived a conductance formula for this hybrid system and clarified that the slope of the dispersion of the chiral edge mode is tunable by the gate voltage applied on the TI [27]. The derivation of the conductance formula is useful to capture the low energy charge transport in newly developed designed topological superconductors and superconducting TIs [28, 29].

The AIII-class topological insulator has a winding number

in one dimension, as shown in the topological periodic table [30]. By inducing the  $s$ -wave pair potential on an AIII-class TI, this system becomes a topological superconductor belonging to the BDI-class, which is characterized by the topological number  $\mathcal{N}$  [31]. The phase diagram of this BDI topological superconductor is shown in Fig. 1. The present BDI topological

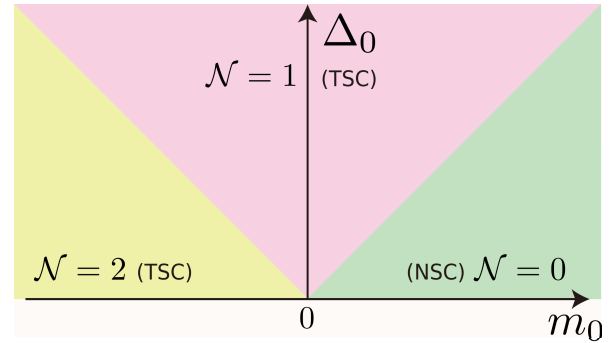


FIG. 1. Phase diagram of BDI topological superconductor [31, 32]

superconductor can be regarded as a one-dimensional version of the quantum anomalous Hall/superconductor hybrid system [32]. Since there are many researches about Quantum anomalous Hall / superconductor hybrid systems [33–37], to clarify the BDI superconductor has a sufficient value. It is remarkable that topological phase transition is tunable by changing the so-called mass parameter defined in the AIII topological insulator model, where a topological insulator is realized for  $m < 0$  [32]. The number of edge modes, SABSs, in this BDI-class topological superconductor coincides with  $\mathcal{N}$  [31, 32]. The zero-temperature conductance at zero voltage shows a noteworthy feature. For the  $\mathcal{N} = 1$  state, the SABS appears as the single mode of the Majorana fermion; thus, the resulting charge conductance becomes  $2e^2/h$  [31, 38]. Meanwhile, for  $\mathcal{N} = 2$ , although the ZESABS exists as two Majorana fermions, because of the destructive interference between two Majorana fermions, the zero-bias conductance becomes zero [31, 38]. Simultaneously, the reflection coefficients of the Andreev reflection disappear. Although several theoretical studies have been done regarding this system [31, 38], they are based on a low-energy effective model or numerical calcula-

tions in a finite system, and the charge conductance formula has not been derived analytically. It is beneficial to solve the scattering problem of a normal metal/one-dimensional (1D) BDI superconductor junction analytically and derive a conductance formula similar to other topological superconductors [27, 28].

The aim of this study was to solve the Bogoliubov-de Gennes (BdG) equation of a normal metal/BDI superconductor junction based on the AIII TI in one dimension. We selected a standard normal metal with parabolic dispersion. We analytically obtained both the normal reflection coefficient  $R_{\sigma\sigma'}$  and Andreev reflection coefficient  $A_{\sigma\sigma'}$ . Here,  $\sigma$  is a spin index of a reflected electron (hole) for a normal (Andreev) reflection, and  $\sigma'$  is a spin index of an injected electron. The resulting conductance shows a wide variety of line shapes. For the  $\mathcal{N} = 0$  state, the conductance exhibits a gap-like structure without sharp coherence peaks in contrast to the standard  $U$ -shaped line shape of differential conductance in tunneling spectroscopy of an  $s$ -wave superconductor. For the  $\mathcal{N} = 1$  state,  $\sum_{\sigma\sigma'} R_{\sigma\sigma'} = \sum_{\sigma\sigma'} A_{\sigma\sigma'}$  is satisfied and the charge conductance has a quantized ZBCP of peak height  $2e^2/h$ . The width of this peak depends on the magnitude of  $m_0$  and  $\Delta_0$ . For the  $\mathcal{N} = 2$  state, the charge conductance has a ZBCP splitting at  $eV = 0$  and becomes zero; this is consistent with previous results. Further, we clarified the spin rotation at zero bias voltage  $eV = 0$ , when the quantization axis of the spin is along the  $z$ -axis. For the  $\mathcal{N} = 1$  state, the spin direction of the normal-reflected electron and Andreev-reflected hole is directed along the  $y$ -axis. Meanwhile, for the  $\mathcal{N} = 2$  state, the Andreev reflection is absent and the spin rotation angle can become  $180^\circ$  for the normal-reflected electron.

The remainder of this paper is organized as follows. In section 2, we present the theory and the method to derive the conductance formula. In section 3, we detail the resulting conductance. In section 4, we demonstrate the spin rotation from the obtained reflection coefficients. Our results are summarized in section 5.

## II. FORMULATION

We consider a normal metal/BDI superconductor (N/BDI) junction, as shown in Fig. 2 [31]. The one-dimensional limit

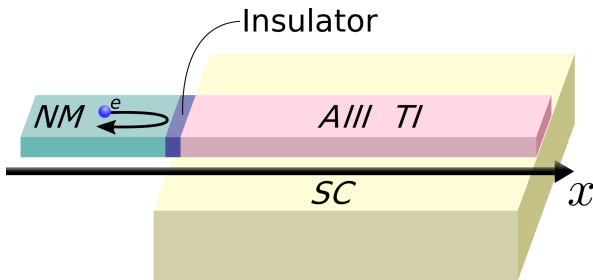


FIG. 2. Normal metal/BDI superconductor junction. BDI superconductor is realized in the AIII topological insulator region that is proximity coupled with a spin-singlet  $s$ -wave superconductor [31].

of a quantum anomalous Hall/superconductor hybrid system can be regarded as a BDI superconductor. The Hamiltonian is given by

$$H = H_N\theta(-x) + U\delta(x) + H_{SC}\theta(x), \quad (1)$$

where  $\theta(x)$  and  $\delta(x)$  are the Heaviside step function and delta function, respectively. The second term indicates the barrier potential with barrier parameter  $U$ .

The Hamiltonian of a normal metal is defined as a standard free electron model with parabolic dispersion.

$$H_N(k) = \left( \frac{\hbar^2}{2m_N} k^2 - \mu \right) \tau_z, \quad (2)$$

where  $\mu$ ,  $m_N$ , and  $\tau_z$  are the chemical potential, effective mass of the normal metal, and Pauli matrices in the Nambu space. Subsequently, the Fermi wave number is given by  $k_F = \sqrt{2m_N\mu/\hbar^2}$ . The Hamiltonian of the BDI superconductor is

$$H_{SC}(k) = \begin{pmatrix} h_{AIII}(k) & i\sigma_y\Delta_0 \\ -i\sigma_y\Delta_0 & -h_{AIII}^*(-k) \end{pmatrix}, \quad (3)$$

$$h_{AIII}(k) = m(k)\sigma_z + A_0k\sigma_x, \quad m(k) = m_0 + B_0k^2, \quad (4)$$

where  $h_{AIII}(k)$  is the AIII-class TI.  $A_0$  and  $B_0$  are material parameters.  $\Delta_0$  is the pair potential of the spin-singlet  $s$ -wave superconductor. Here,  $m_0$ ,  $\sigma_z$ , and  $A_0$  denote the effective mass,  $z$  component of the Pauli matrix, and spin-orbital coupling, respectively. Herein, the chemical potential of the AIII-class insulator is fixed at zero. Therefore, the Fermi level is located in the middle between the conduction and valence band. For  $m_0 < 0$ , the AIII-class insulator becomes a topological hosting edge state [31, 32].

We normalize each parameter using  $k_F$  in the remainder of this paper

$$\begin{cases} \tilde{m}_0 &= m_0/\mu \\ \tilde{\Delta}_0 &= \Delta_0/\mu \end{cases} \quad \begin{cases} A &= A_0/\left(\frac{\hbar^2 k_F}{2m_N}\right) \\ B &= B_0/\left(\frac{\hbar^2}{2m_N}\right) \\ Z &= 2U/\left(\frac{\hbar^2 k_F}{2m_N}\right) \end{cases}. \quad (5)$$

The eigenenergy  $E_{\pm}$  and eigenfunction  $\psi_{\pm}(k)$  of  $H_{SC}$  are obtained:

$$E_{\pm} = \sqrt{A_0^2 k^2 + (m(k) \pm \Delta_0)^2} \quad (6)$$

$$\psi_{\pm}(k) = \begin{pmatrix} 1 \\ Q_{\pm}(k) \\ \pm Q_{\pm}(k) \\ \pm 1 \end{pmatrix}, \quad Q_{\pm}(k) = -\frac{m(k) \pm \Delta_0 - E}{A_0 k}. \quad (7)$$

We can confirm that the bulk energy gap of the BDI superconductor closes at  $m_0 = \pm\Delta_0$ , as calculated from the eigenenergy. Thus, the topological phase transition occurs at  $m_0 = \pm\Delta_0$ .

In the following section, we study the scattering problem of the N/BDI junction. We assume that the spin direction of an injected electron is along the  $z$  axis. In the 1D BDI superconductor, the wave function is satisfied, as follows:

$$\Psi_N(x) = \Psi_{in}(x) + \Psi_{ref}(x) \quad (x < 0) \quad (8)$$

$$\Psi_{SC}(x) = \Psi_{tra}(x) \quad (x > 0) \quad (9)$$

$$\Psi_{\text{in}} = \begin{pmatrix} \delta_{\uparrow\sigma} \\ \delta_{\downarrow\sigma} \\ 0 \\ 0 \end{pmatrix} e^{ik_{\text{F}}x}, \quad \Psi_{\text{ref}} = \begin{pmatrix} b_{\uparrow\sigma} \\ b_{\downarrow\sigma} \\ 0 \\ 0 \end{pmatrix} e^{-ik_{\text{F}}x} + \begin{pmatrix} 0 \\ 0 \\ a_{\uparrow\sigma} \\ a_{\downarrow\sigma} \end{pmatrix} e^{ik_{\text{F}}x}, \quad (10)$$

$$\Psi_{\text{tra}} = t_{1+}\psi_{\pm}(k_{1+})e^{ik_{1+}x} + t_{2+}\psi_{\pm}(k_{2+})e^{ik_{2+}x} \\ + t_{1-}\psi_{\pm}(k_{1-})e^{ik_{1-}x} + t_{2-}\psi_{\pm}(k_{2-})e^{ik_{2-}x}, \quad (11)$$

where  $\sigma$  is the spin of an injected electron;  $b_{\sigma'\sigma}$  and  $a_{\sigma'\sigma}$  are the amplitudes of the normal and Andreev reflections with  $\sigma' = \uparrow (\downarrow)$ ;  $t_{1\pm}$  and  $t_{2\pm}$  are the corresponding transmission amplitudes. The wave number in the BDI superconductor is calculated from the eigenenergy:  $E_{\pm}$

$$(k_{1,\pm}(E))^2 = \frac{1}{2B_0^2} \left( -2B_0(m_0 \pm \Delta_0) + A_0^2 \right) \\ + \sqrt{A_0^4 + 4B_0(m_0 \pm \Delta_0)A_0^2 + 4B_0^2E^2} \quad (12)$$

$$(k_{2,\pm}(E))^2 = \frac{1}{2B_0^2} \left( -2B_0(m_0 \pm \Delta_0) + A_0^2 \right) \\ - \sqrt{A_0^4 + 4B_0(m_0 \pm \Delta_0)A_0^2 + 4B_0^2E^2}, \quad (13)$$

where  $E$  is the energy measured from the Fermi level. The sign of the wave number is determined by the group velocity such that the wave function does not diverge for  $x \rightarrow \infty$ . The boundary condition of the wave function at  $x = 0$  is given as follows:

$$\begin{cases} \Psi_{\text{SC}}(x=0) - \Psi_{\text{N}}(x=0) = 0 \\ \hbar(\hat{v}_{\text{SC}} \{\Psi_{\text{SC}}(x)\}|_{x=+0} - \hat{v}_{\text{N}} \{\Psi_{\text{N}}(x)\}|_{x=-0}) \\ = -2iU\tau_z \Psi_{\text{N}}(x=0) \end{cases} \quad (14)$$

Here,  $\hat{v}$  is the velocity operator  $\hat{v} = \frac{1}{\hbar} \frac{\partial H}{\partial (-i\partial_x)}$ .

### III. TUNNELING EFFECT

The charge conductance  $\Gamma$  in the N/BDI junction can be expressed using the reflection coefficients

$$\Gamma = \frac{e^2}{h} \left( 2 - \sum_{\sigma, \sigma'} (R_{\sigma\sigma'} - A_{\sigma\sigma'}) \right). \quad (15)$$

The amplitude of the normal reflection  $\mathbf{b}_{\sigma} = (b_{\uparrow\sigma}, b_{\downarrow\sigma})$  and that of the Andreev reflection  $\mathbf{a}_{\sigma} = (a_{\uparrow\sigma}, a_{\downarrow\sigma})$  for an injected electron with  $\sigma = \uparrow, \downarrow$  are expressed by two component vectors

obtained from the boundary condition (14)

$$\mathbf{b}_{\sigma} = \left( \mathbf{I} + iZ \left\{ \left( \hat{\mathbf{K}}_{+} + \gamma^* \mathbf{I} \right)^{-1} + \left( \hat{\mathbf{K}}_{-} + \gamma^* \mathbf{I} \right)^{-1} \right\} \right)^{-1} \\ \left( \mathbf{I} - \gamma^* \left\{ \left( \hat{\mathbf{K}}_{+} + \gamma^* \mathbf{I} \right)^{-1} + \left( \hat{\mathbf{K}}_{-} + \gamma^* \mathbf{I} \right)^{-1} \right\} \right) \mathbf{u}_{\sigma} \quad (16)$$

$$\mathbf{a}_{\sigma} = -2\sigma_x \left( \mathbf{I} + iZ \left\{ \left( \hat{\mathbf{K}}_{+} + \gamma \mathbf{I} \right)^{-1} + \left( \hat{\mathbf{K}}_{-} + \gamma \mathbf{I} \right)^{-1} \right\} \right)^{-1} \\ \left( \left\{ \left( \hat{\mathbf{K}}_{+} + \gamma \mathbf{I} \right)^{-1} - \left( \hat{\mathbf{K}}_{-} + \gamma \mathbf{I} \right)^{-1} \right\} \right) \mathbf{u}_{\sigma}, \quad (17)$$

with  $\mathbf{u}_{\sigma} = (\delta_{\uparrow\sigma}, \delta_{\downarrow\sigma})$ . Here,  $\gamma \equiv 2 + iZ$  with the barrier parameter  $Z$ ,  $\mathbf{I}$  is a  $2 \times 2$  unit matrix, and  $\hat{\mathbf{K}}_{\pm}$  is a  $2 \times 2$  matrix with respect to the wave number (12)(13) using the factor of the wave function (7).

$$\hat{\mathbf{K}}_{\pm} \equiv A\sigma_x + 2B\sigma_z \hat{\mathbf{Q}}_{\pm} \begin{pmatrix} k_{1\pm}/k_{\text{F}} & 0 \\ 0 & k_{2\pm}/k_{\text{F}} \end{pmatrix} \hat{\mathbf{Q}}_{\pm}^{-1} \quad (18)$$

$$\hat{\mathbf{Q}}_{\pm} \equiv \begin{pmatrix} 1 & 1 \\ Q_{\pm}(k_{1\pm}) & Q_{\pm}(k_{2\pm}) \end{pmatrix}. \quad (19)$$

The matrices of the reflection coefficients of the normal reflection  $R_{\sigma\sigma'}$  and that of the Andreev reflection  $A_{\sigma\sigma'}$  are given by

$$R_{\sigma\sigma'} = \begin{pmatrix} |b_{\uparrow\uparrow}|^2 & |b_{\uparrow\downarrow}|^2 \\ |b_{\downarrow\uparrow}|^2 & |b_{\downarrow\downarrow}|^2 \end{pmatrix} \quad (20)$$

$$A_{\sigma\sigma'} = \begin{pmatrix} |a_{\uparrow\uparrow}|^2 & |a_{\uparrow\downarrow}|^2 \\ |a_{\downarrow\uparrow}|^2 & |a_{\downarrow\downarrow}|^2 \end{pmatrix}, \quad (21)$$

We calculate the conductance  $\Gamma$  analytically with bias voltage  $V$  where  $E = eV$  is satisfied. We selected various mass parameters  $m_0$  for a fixed  $\Delta_0$ , as shown in Fig.3. For  $\mathcal{N} = 0$  cases, the obtained conductance never becomes exactly zero for any  $V$  ( $\Gamma \neq 0$ ) owing to the Andreev reflection. The sharp coherent peaks that appear in the case of conventional tunneling spectroscopy of the  $s$ -wave superconductor is absent in the conductance. This is because the spin-singlet  $s$ -wave pair potential is induced in the insulating AIII phase. The conductance shows a two-gap behavior at  $eV = |m_0 \pm \Delta_0|$ . For the  $\mathcal{N} = 1$  state, the ZBCP appears with its peak height of  $2e^2/h$ . The peak width is determined by the barrier parameter  $Z$  and gap width  $W_-$ , which is the gap width of the energy band  $E_-$  defined in eq. (6)

$$W_- = \begin{cases} |m_0 - \Delta_0| & (m_0 - \Delta_0 > -A_0^2/2B_0) \\ \sqrt{\frac{A_0^2}{B_0} \left( |m_0 - \Delta_0| - \frac{A_0^2}{4B_0} \right)} & (m_0 - \Delta_0 < -A_0^2/2B_0) \end{cases}. \quad (22)$$

When  $m_0$  decreases,  $W_-$  increases in  $\mathcal{N} = 1$  phase, and peak width, which is approximately proportional to  $W_-$ , also increases (Fig.3(c)). At  $m_0 = \Delta_0$ , the width of the peak becomes zero and the energy spectrum of the BDI superconductor becomes gapless corresponding to a topological transition. This

ZBCP is due to the ZESABS that manifests as a Majorana fermion at the edge of the BDI superconductor [31, 32]. For the  $\mathcal{N} = 2$  state, the charge conductance exhibits a ZBCP splitting. The height of the peaks at a nonzero voltage is suppressed with the decrease in the value of  $m_0$ . At  $eV = 0$ , the conductance at zero voltage becomes exactly zero, consistent with previous results [31, 37, 38].

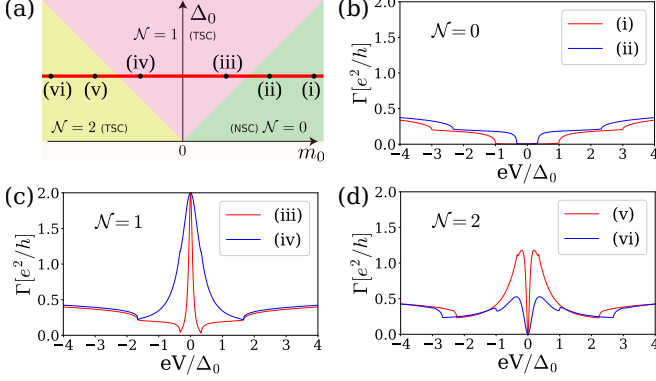


FIG. 3. Calculated conductance for various  $m_0$ . We selected  $\tilde{\Delta}_0 = 0.03$ ,  $A = B = 0.1$ , and  $Z = 1$ . (a): The values of  $(m_0, \Delta_0)$  in the phase diagram of the BDI superconductor. (b):  $\mathcal{N} = 0$  with (i)  $\tilde{m}_0 = 0.06$  and (ii)  $\tilde{m}_0 = 0.04$ . (c):  $\mathcal{N} = 1$  with (iii)  $\tilde{m}_0 = 0.02$  and (iv)  $\tilde{m}_0 = -0.02$ . (d):  $\mathcal{N} = 2$  with (v)  $\tilde{m}_0 = -0.04$  and (vi)  $\tilde{m}_0 = -0.06$ .

### ZERO BIAS VOLTAGE

Next, we focus on the conductance at zero voltage where more compact formula of coefficients of the Andreev and normal reflections and conductance can be available. For convenience, we introduce the following:

$$D_{\pm} \equiv \sqrt{A^2 + 4B(\tilde{m}_0 \pm \tilde{\Delta}_0)}. \quad (23)$$

The amplitudes of both the normal and Andreev reflections can be expressed as

$$\begin{cases} \mathbf{b}_{\sigma} = \frac{(\gamma^2 + D_+ D_-)}{(|\gamma|^2 - D_+ D_-)^2 + 4(D_+ + D_-)^2} \{ (|\gamma|^2 - D_+ D_-) - 2i(D_+ + D_-)\sigma_z \} \mathbf{u}_{\sigma} \\ \mathbf{a}_{\sigma} = -\frac{2(D_+ - D_-)}{(|\gamma|^2 - D_+ D_-)^2 + 4(D_+ + D_-)^2} \{ 2(D_+ + D_-)\sigma_x + (|\gamma|^2 - D_+ D_-)\sigma_y \} \mathbf{u}_{\sigma} \end{cases} \quad (\text{if } \mathcal{N} = 0)$$

$$\begin{cases} \mathbf{b}_{\sigma} = \frac{1}{2} \left\{ \frac{\gamma^2 - D_+^2}{|\gamma|^2 + D_+^2} - \text{sgn}(A_0) \frac{\gamma^2 + D_+^2}{|\gamma|^2 + D_+^2} \sigma_y \right. \\ \left. - i \frac{2\gamma^* D_+}{|\gamma|^2 + D_+^2} \sigma_z \right\} \mathbf{u}_{\sigma} \\ \mathbf{a}_{\sigma} = -\frac{i}{2} \left\{ \text{sgn}(A_0) \frac{2ZD_+}{|\gamma|^2 + D_+^2} + i \frac{|\gamma|^2 - D_+^2}{|\gamma|^2 + D_+^2} \sigma_x \right. \\ \left. - i \frac{4D_+}{|\gamma|^2 + D_+^2} \sigma_y - \text{sgn}(A_0) \sigma_z \right\} \mathbf{u}_{\sigma} \end{cases} \quad (\text{if } \mathcal{N} = 1)$$

$$\begin{cases} \mathbf{b}_{\sigma} = -\frac{1}{\gamma} (iZ + 2\text{sgn}(A_0)\sigma_y) \mathbf{u}_{\sigma} \\ \mathbf{a}_{\sigma} = \mathbf{0} \end{cases} \quad (\text{if } \mathcal{N} = 2). \quad (24)$$

For  $\mathcal{N} = 0$ , both amplitudes of the normal and Andreev reflections exist. For  $\mathcal{N} = 1$ , after some straightforward calculations, we obtain

$$\sum_{\sigma, \sigma'} R_{\sigma\sigma'} = \sum_{\sigma, \sigma'} A_{\sigma\sigma'}. \quad (25)$$

This implies that the contributions of the normal and Andreev reflections are completely balanced. This property is unique although the ZBCP exists in both the Andreev and normal reflections. It is qualitatively different from the previous normal metal/unconventional junctions with the perfect resonant case, where only the Andreev reflection exists at zero voltage [2, 14]. Consequently, differences are observed between the heights of these ZBCPs. For the  $\mathcal{N} = 2$  state, although the ZESABS exists, the Andreev reflection is completely suppressed.

Using the results above, we obtain  $\Gamma$  as follows:

$$\Gamma = \frac{e^2}{h} \times \begin{cases} \frac{16(D_+ - D_-)^2}{(|\gamma|^2 - D_+ D_-)^2 + 4(D_+ + D_-)^2} & (\text{if } \mathcal{N} = 0) \\ 2 & (\text{if } \mathcal{N} = 1) \\ 0 & (\text{if } \mathcal{N} = 2) \end{cases}. \quad (26)$$

For the  $\mathcal{N} = 1$  state, we can demonstrate analytically that the charge conductance becomes  $\frac{2e^2}{h}$ , as shown in Fig.4.

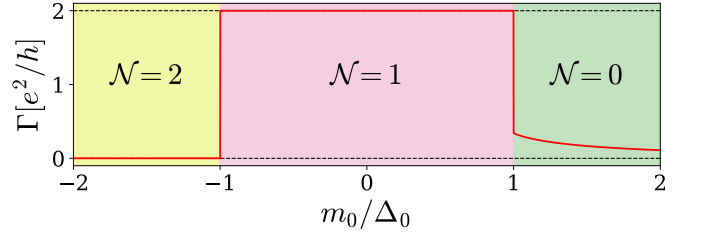


FIG. 4. Conductance with zero bias voltage for  $\tilde{\Delta}_0 = 0.25$ ,  $A = B = 0.1$ ,  $Z = 1$  (Solid line). Dashed lines are the guide for the eye.

### IV. SPIN ROTATION

We have obtained the normal and Andreev reflection coefficients analytically; thus, we can analyze the detailed property of the reflected particles. In this section, we study the spin rotation through the scattering processes at the interface. Here, we consider the normal and Andreev reflections at zero bias voltage to use the formulae in the previous section. Subsequently, the reflection amplitude  $\mathbf{b}_{\sigma}$ ,  $\mathbf{a}_{\sigma}$  is expressed by the spin rotational operator  $\exp\left(i\frac{\hat{\theta}}{2} \cdot \hat{\sigma}\right)$ , where  $\hat{\theta} = \theta\hat{n}$  denotes the rotational axis  $\hat{n}$  and rotational angle  $\theta$ . The results depend highly on the topological phase in the BDI superconductor.

For the  $\mathcal{N} = 1$  state, the reflection coefficients are denoted by a linear combination of spinors that are expressed by two types of spin rotations

$$\begin{cases} \mathbf{b}_{\sigma} = \frac{1}{2} \left\{ \exp\left(i\frac{\hat{\theta}_{1b1}}{2} \cdot \hat{\sigma}\right) - i \exp\left(i\frac{\hat{\theta}_{1b2}}{2} \cdot \hat{\sigma}\right) \right\} \mathbf{u}_{\sigma} \\ \mathbf{a}_{\sigma} = \frac{\text{sgn}(A)}{2} \left\{ \exp\left(i\frac{\pi}{2}\sigma_z\right) - i \exp\left(i\frac{\hat{\theta}_{1a}}{2} \cdot \hat{\sigma}\right) \right\} \mathbf{u}_{\sigma} \end{cases} \quad (\text{if } \mathcal{N} = 1), \quad (27)$$

where the rotation angles are as follows:

$$\hat{\theta}_{1b1}/2 = \arctan \left( \frac{4\sqrt{Z^2 + D_+^2}}{4 - Z^2 - D_+^2} \right) \left( \begin{array}{c} 0 \\ \text{sgn}(A)Z \\ -D_+ \end{array} \right) \left/ \left( \begin{array}{c} 0 \\ \text{sgn}(A)Z \\ -D_+ \end{array} \right) \right. \quad (28)$$

$$\hat{\theta}_{1b2}/2 = \arctan \left( -\frac{\sqrt{(4 - Z^2 + D_+^2)^2 + 4Z^2 D_+^2}}{4Z} \right) \left( \begin{array}{c} 0 \\ (4 - Z^2 + D_+^2)\text{sgn}(A) \\ 2ZD_+ \end{array} \right) \left/ \left( \begin{array}{c} 0 \\ (4 - Z^2 + D_+^2)\text{sgn}(A) \\ 2ZD_+ \end{array} \right) \right. \quad (29)$$

$$\hat{\theta}_{1a}/2 = \arctan \left( \text{sgn}(A) \frac{\sqrt{|\gamma|^4 + 2D_+^2(4 - Z^2) + D_+^4}}{2ZD_+} \right) \left( \begin{array}{c} |\gamma|^2 - D_+^2 \\ -4D_+ \\ 0 \end{array} \right) \left/ \left( \begin{array}{c} |\gamma|^2 - D_+^2 \\ -4D_+ \\ 0 \end{array} \right) \right. \quad (30)$$

Fig.5 shows the spin direction of the normal and Andreev reflections with the injection of an up-spin electron, where  $\theta_y$  and  $\phi_{xz}$  are the polar angle from the  $y$ -axis and the azimuth angle in the  $xz$ -plane, respectively. In the case of  $A > 0$ , the spin direction for both the normal and Andreev reflections are almost along the direction of  $-\hat{y}$  because of  $\theta_y \sim \pi$  for any  $Z$ , as shown in Fig.5(a). Here,  $\hat{y}$  is a unit vector along the  $y$ -direction. Meanwhile, the spin directions are the opposite in the  $A < 0$  case. This implies that the spin direction of the reflected waves depends on that of the BDI superconductor which couples to the momentum by the spin-orbit coupling. Additionally, we confirm that the spin direction for the normal and Andreev reflections with a down-spin injection is the same as those for an up-spin injection. In other words, the spin directions of the reflected waves are polarized both in the electron and hole sectors. This spin polarization phenomenon is caused by the spin-orbit coupling of the BDI superconductor.

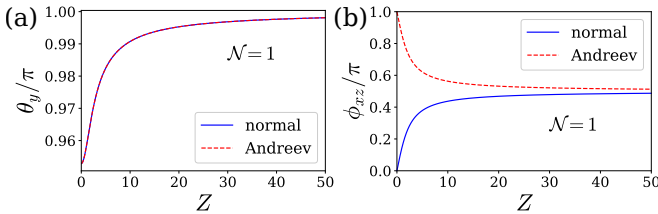


FIG. 5. Calculated spin rotation for  $\mathcal{N} = 1$  at  $eV = 0$ . We selected  $\tilde{\Delta}_0 = 0.03$ ,  $A = B = 0.1$ ,  $\tilde{m}_0 = 0$  and  $Z = 1$ . (a): Plot of  $\theta_y$  that is the polar angle of the spin direction from the  $y$ -axis. The normal and Andreev reflections has the same  $\theta_y$  value. (b): Plot of  $\phi_{xz}$  that is the azimuth angle of the spin direction in the  $xz$ -plane.

For the  $\mathcal{N} = 2$  state, the reflection amplitudes are denoted as follows:

$$\begin{cases} \mathbf{b}_\sigma &= R_{2b} \exp \left( i \frac{\hat{\theta}_{2b}}{2} \cdot \hat{\sigma} \right) \mathbf{u}_\sigma \\ \mathbf{a}_\sigma &= \mathbf{0} \end{cases} \quad (\text{if } \mathcal{N} = 2), \quad (31)$$

where the coefficient and rotation angle are as follows:

$$R_{2b} = -i \frac{2 - iZ}{\sqrt{4 + Z^2}}, \quad \hat{\theta}_{2b}/2 = \arctan \left( -\text{sgn}(A) \frac{2}{Z} \right) \begin{pmatrix} 0 \\ 1 \\ 0 \end{pmatrix}. \quad (32)$$

According to Eq.(32), normal reflection depends only on the sign of  $A$  and does not depend on other parameters of the BDI superconductor. Fig.6 shows the spin direction of the normal reflection in an up-spin injection, where  $\theta_z$  and  $\phi_{xy}$  are the polar angle from the  $z$ -axis and the azimuth angle in the  $xy$ -plane, respectively. As shown in Fig.6(a), the spins of the reflections are directed to  $-\hat{z}$ , i.e.,  $\pi$ -rotation at  $Z = 0$ , but do not change through the scattering for  $Z = \infty$ . Here,  $\hat{z}$  is a unit vector. This is because the couplings between the injected electron and the edge state of the BDI becomes weak with increasing barrier strength. From  $Z = 0$  to  $\infty$ , the spin direction of the normal reflection rotates in the  $xz$ -plane. It is noteworthy that the azimuth angle depends on the sign of  $A$ , as shown in Fig.6(b). It is known that a giant spin rotation appears in the normal metal/quantum spin Hall junction depending on the edge states[39]. Similarly, spin rotations appear for a weak barrier strength.

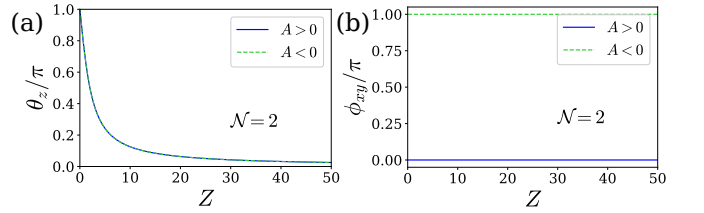


FIG. 6. Calculated spin rotation injected up-spin for  $\mathcal{N} = 2$  at  $eV = 0$ . We selected  $\Delta_0 = 0.03$ ,  $A = B = 0.1$ , and  $Z = 1$ . (a): Plot of  $\theta_z$  that is the polar angle of the spin direction from the  $z$ -axis. In the  $A > 0$  and  $A < 0$  cases, the same value is observed for  $\theta_z$ . (b): Plot of  $\phi_{xy}$  that is the azimuth angle of the spin direction in the  $xy$ -plane.

Finally, for the  $\mathcal{N} = 0$  state, the reflection amplitudes are expressed as follows:

$$\begin{cases} \mathbf{b}_\sigma &= R_{0b} \exp \left( i \frac{\hat{\theta}_{0b}}{2} \cdot \hat{\sigma} \right) \mathbf{u}_\sigma \\ \mathbf{a}_\sigma &= R_{0a} \exp \left( i \frac{\hat{\theta}_{0a}}{2} \cdot \hat{\sigma} \right) \mathbf{u}_\sigma \end{cases} \quad (\text{if } \mathcal{N} = 0), \quad (33)$$

where the coefficients and rotation angles are as follows:

$$\begin{cases} R_{0b} &= \frac{\gamma^{*2} + D_+ D_-}{\sqrt{(|\gamma|^2 - D_+ D_-)^2 + 4(D_+ + D_-)^2}} \\ \hat{\theta}_{0b}/2 &= \arctan \left( \frac{2(D_+ + D_-)}{|\gamma|^2 - D_+ D_-} \right) \begin{pmatrix} 0 \\ 0 \\ 1 \end{pmatrix} \\ R_{0a} &= \frac{2i(D_+ - D_-)}{\sqrt{(|\gamma|^2 - D_+ D_-)^2 + 4(D_+ + D_-)^2}} \\ \hat{\theta}_{0a}/2 &= \frac{\pi}{2} \begin{pmatrix} 2(D_+ + D_-) \\ 0 \\ 0 \end{pmatrix} \left/ \left( \begin{pmatrix} 2(D_+ + D_-) \\ 0 \\ 0 \end{pmatrix} \right) \right. \end{cases} \quad (34)$$

$$\begin{cases} R_{0a} &= \frac{2i(D_+ - D_-)}{\sqrt{(|\gamma|^2 - D_+ D_-)^2 + 4(D_+ + D_-)^2}} \\ \hat{\theta}_{0a}/2 &= \frac{\pi}{2} \begin{pmatrix} 2(D_+ + D_-) \\ 0 \\ 0 \end{pmatrix} \left/ \left( \begin{pmatrix} 2(D_+ + D_-) \\ 0 \\ 0 \end{pmatrix} \right) \right. \end{cases} \quad (35)$$

When the spin direction for the injected electrons is along the  $\hat{z}$ -axis, any spin flipping or rotation does not appear because  $\theta_{ob}$  directs  $\hat{z}$  and the rotational axis is along the  $z$ -axis. Further, the Andreev reflection is flipped simply, i.e.,  $\uparrow$  to  $\downarrow$  or vice versa. This spin rotation is similar to that of conventional tunneling of the  $s$ -wave superconductor. The results above are summarized in Table I.

TABLE I. Spin direction of the normal and Andreev reflections with injected up-spin electron.  $\hat{y}$  and  $\hat{z}$  are unit vectors

$\mathcal{N}$	Normal		Andreev	
	$Z = 0$	$Z = \infty$	$Z = 0$	$Z = \infty$
0	$+\hat{z}$	$+\hat{z}$	$-\hat{z}$	$-\hat{z}$
1	$-\text{sgn}(A)\hat{y}$	$-\text{sgn}(A)\hat{y}$	$-\text{sgn}(A)\hat{y}$	$-\text{sgn}(A)\hat{y}$
2	$-\hat{z}$	$+\hat{z}$	-	-

## V. CONCLUSION

We have studied the tunneling effect in a topological superconductor based on a 1D AIII-class TI that is proximity coupled with a spin-singlet  $s$ -wave superconductor. This topological superconductor belongs to the BDI-class and topologically different phases are characterized by the topological invariant  $\mathcal{N}$  for a bulk BDI superconductor. By solving the BdG equation of the normal metal/BDI superconductor junction, we have analytically obtained both the normal reflection coefficient  $R_{\sigma\sigma'}$  and Andreev reflection coefficient  $A_{\sigma\sigma'}$ , where  $\sigma(\sigma')$  is a spin index of the reflected (injected) wave. The resulting conductance indicates a wide variety of line shapes.

For the  $\mathcal{N} = 0$  state, the obtained conductance exhibits a Gap-like structure without sharp coherence peaks at their maxima, in contrast to the standard  $U$ -shaped line shape in  $s$ -wave superconductor tunneling spectroscopy. For the  $\mathcal{N} = 1$  state,  $\sum_{\sigma\sigma'} R_{\sigma\sigma'} = \sum_{\sigma\sigma'} A_{\sigma\sigma'}$  is satisfied. The obtained conductance exhibits a ZBCP of height  $2e^2/h$ . The width of this peak depends on the magnitudes of  $m_0$  and  $\Delta_0$ . With the decrease in the value of  $m_0$  for a fixed  $\Delta_0$ , the width of the peak increases up to  $m_0 = -\Delta_0$ . For the  $\mathcal{N} = 2$  state, the charge conductance exhibits a ZBCP spitting; at  $eV = 0$ , it became zero, consistent with previous results. Further, we have calculated the spin rotation at zero bias voltage  $eV = 0$ , when the quantization axis of the spin is along the  $z$ -axis. For the  $\mathcal{N} = 0$  state, the spin direction of the reflected electron is along the  $z$ -axis and that of the hole is in the opposite direction. For the  $\mathcal{N} = 1$  state, the spin directions of the reflected electron and hole are directed along the  $y$ -axis. Meanwhile, for the  $\mathcal{N} = 2$  state,  $A_{\sigma\sigma'} = 0$  is always satisfied and the reflected electron exhibited a spin rotation. The spin rotation angle can become  $180^\circ$  in the extreme case when no barrier exists at the boundary.

## ACKNOWLEDGMENTS

We would like to thank valuable discussion with A. Yamage. This work was supported by Grant-in-Aid for Scientific Research on Innovative Areas, Topological Material Science (Grant Nos. JP15H05851, JP15H05853) and JSPS KAKENHI Grant Numbers JP18K03538 and JP18H01176 from the Ministry of Education, Culture, Sports, Science, and Technology, Japan (MEXT).

- 
- [1] G. E. Blonder, M. Tinkham, and T. Klapwijk: Phys. Rev. B **25** (1982) 4515.
- [2] Y. Tanaka and S. Kashiwaya: Phys. Rev. Lett. **74** (1995) 3451.
- [3] Y. Tanaka and S. Kashiwaya: Phys. Rev. B **53** (1996) 9371.
- [4] S. Kashiwaya, Y. Tanaka, M. Koyanagi, H. Takashima, and K. Kajimura: Phys. Rev. B **51** (1995) 1350.
- [5] S. Kashiwaya, Y. Tanaka, N. Terada, M. Koyanagi, S. Ueno, L. Alff, H. Takashima, Y. Tanuma, and K. Kajimura: J. Phys. Chem. Solid **59** (1998) 2034.
- [6] M. Covington, M. Aprili, E. Paraoanu, L. H. Greene, F. Xu, J. Zhu, and C. A. Mirkin: Phys. Rev. Lett. **79** (1997) 277.
- [7] L. Alff, H. Takashima, S. Kashiwaya, N. Terada, H. Ihara, Y. Tanaka, M. Koyanagi, and K. Kajimura: Phys. Rev. B **55** (1997) R14757.
- [8] J. Y. T. Wei, N.-C. Yeh, D. F. Garrigus, and M. Strasik: Phys. Rev. Lett. **81** (1998) 2542.
- [9] A. Biswas, P. Fournier, M. M. Qazilbash, V. N. Smolyaninova, H. Balci, and R. L. Greene: Phys. Rev. Lett. **88** (2002) 207004.
- [10] B. Chesca, H. J. H. Smilde, and H. Hilgenkamp: Phys. Rev. B **77** (2008) 184510.
- [11] L. J. Buchholtz and G. Zwirnagl: Phys. Rev. B **23** (1981) 5788.
- [12] J. Hara and K. Nagai: Prog. Theor. Phys. **76** (1986) 1237.
- [13] C. R. Hu: Phys. Rev. Lett. **72** (1994) 1526.
- [14] S. Kashiwaya and Y. Tanaka: Rep. Prog. Phys. **63** (2000) 1641.
- [15] T. Löfwander, V. S. Shumeiko, and G. Wendin: Supercond. Sci. Technol. **14** (2001) R53.
- [16] M. Yamashiro, Y. Tanaka, and S. Kashiwaya: Phys. Rev. B **56** (1997) 7847.
- [17] M. Yamashiro, Y. Tanaka, Y. Tanuma, and S. Kashiwaya: J. Phys. Soc. Jpn. **67** (1998) 3224.
- [18] H. Kwon, K. Sengupta, and V. Yakovenko: Eur. Phys. J. B **37** (2004) 349.
- [19] Z. Mao, K. Nelson, R. Jin, Y. Liu, and Y. Maeno: Phys. Rev. Lett. **87** (2001) 037003.
- [20] S. Kashiwaya, H. Kashiwaya, H. Kambara, T. Furuta, H. Yaguchi, Y. Tanaka, and Y. Maeno: Phys. Rev. Lett. **107** (2011) 077003.
- [21] Y. Maeno, H. Hashimoto, K. Yoshida, S. Nishizaki, T. Fujita, J. G. Bednorz, and F. Lichtenberg: Nature **372** (1994) 532.
- [22] A. P. Mackenzie and Y. Maeno: Rev. Mod. Phys. **75** (2003) 657.
- [23] M. Sato, Y. Tanaka, K. Yada, and T. Yokoyama: Phys. Rev. B **83** (2011) 224511.
- [24] G.E. Volovik: JETP Lett. **66** (1997) 522.
- [25] A. Furusaki, M. Matsumoto, and M. Sigrist: Phys. Rev. B **64** (2001) 054514.
- [26] Y. Tanaka, M. Sato, and N. Nagaosa: J. Phys. Soc. Jpn. **81** (2012) 011013.

- [27] Y. Tanaka, T. Yokoyama, and N. Nagaosa: *Phys. Rev. Lett.* **103** (2009) 107002.
- [28] S. Takami, K. Yada, A. Yamakage, M. Sato, and Y. Tanaka: *J. Phys. Soc. Jpn.* **83** (2014) 064705.
- [29] C. Reeg and D. L. Maslov: *Phys. Rev. B* **95** (2017) 205439.
- [30] A. P. Schnyder, S. Ryu, A. Furusaki, and A. W. W. Ludwig: *Phys. Rev. B* **78** (2008) 195125.
- [31] J. J. He, J. Wu, T.-P. Choy, X.-J. Liu, Y. Tanaka, and K. T. Law: *Nature Communications* **5** (2014) 3232.
- [32] X. L. Qi, T. L. Hughes, and S. C. Zhang: *Phys. Rev. B* **82** (2010) 184516.
- [33] W. Ji and X.-G. Wen: *Phys. Rev. Lett.* **120** (2018) 107002.
- [34] Y. Huang, F. Setiawan, and J. D. Sau: *Phys. Rev. B* **97** (2018) 100501.
- [35] Q. L. He, L. Pan, A. L. Stern, E. C. Burks, X. Che, G. Yin, J. Wang, B. Lian, Q. Zhou, E. S. Choi, K. Murata, X. Kou, Z. Chen, T. Nie, Q. Shao, Y. Fan, S.-C. Zhang, K. Liu, J. Xia, and K. L. Wang: *Science* **357** (2017) 294.
- [36] A. Ii, K. Yada, M. Sato, and Y. Tanaka: *Phys. Rev. B* **83** (2011) 224524.
- [37] A. Ii, A. Yamakage, K. Yada, M. Sato, and Y. Tanaka: *Phys. Rev. B* **86** (2012) 174512.
- [38] A. Yamakage and M. Sato: *Physica E: Low-dimensional Systems and Nanostructures* **55** (2014) 13 .
- [39] T. Yokoyama, Y. Tanaka, and N. Nagaosa: *Phys. Rev. Lett.* **102** (2009) 166801.